

Photofission of Heavy Nuclei at Energies up to 4 GeV

C. Cetina, B. L. Berman, W. J. Briscoe, P. L. Cole,* G. Feldman, P. Heimberg, L. Y. Murphy,
S. A. Philips, and J. C. Sanabria†

Center for Nuclear Studies, Department of Physics, The George Washington University, Washington, D.C. 20052

Hall Crannell, A. Longhi, and D. I. Sober

Department of Physics, The Catholic University of America, Washington, D.C. 20064

G. Ya. Kezerashvili‡

Budker Institute of Nuclear Physics, 630090 Novosibirsk, Russia

(Received 27 December 1999)

Total photofission cross sections for ^{238}U , ^{235}U , ^{233}U , ^{237}Np , ^{232}Th , and $^{\text{nat}}\text{Pb}$ have been measured *simultaneously*, using tagged photons in the energy range $E_\gamma = 0.17\text{--}3.84$ GeV. This was the first experiment performed using the Photon Tagging Facility in Hall B at Jefferson Lab. Our results show that the photofission cross section for ^{238}U relative to that for ^{237}Np is about 80% over the entire energy range, implying the presence of important processes which compete with fission. If we assume that for ^{237}Np the photofission probability is equal to unity, we observe a significant shadowing effect, starting below 1.5 GeV.

PACS numbers: 25.85.Jg, 25.20.Dc, 27.90.+b

It has long been assumed [1,2] that the photofission cross section $\sigma_{\gamma F}$ for the uranium and transuranic isotopes should exhaust the total nuclear photoabsorption cross section $\sigma_{\gamma A}$ for incident photon energies above 50 MeV, so that the fission probability of these nuclei at these energies was generally assumed to be unity. If this were the case, the photofission method would provide a very convenient way to determine the total photoabsorption cross section. This interesting quantity [3], not easily determined by other methods for heavy nuclei, would yield information on the intrinsic properties of nucleons inside the nuclear medium, as well as on the hadronic nature of the photon.

One might assume the total photoabsorption cross section per nucleon $\sigma_{\gamma A}/A$ to be independent of A . In the Δ -resonance region, this has been shown to be plausible by various measurements for several complex nuclei ranging from Li to U, leading to the concept of the “universal curve” [4]. For several nuclei, recent measurements have been performed up to 2.6 GeV [5]. If we define the photofissility W_F of a nucleus as the probability that this nucleus undergoes fission, then we can express W_F as the ratio $\sigma_{\gamma F}/\sigma_{\gamma A}$. A constant $\sigma_{\gamma A}/A$ implies that, for two nuclei, the ratio of their photofissilities is given by the ratio of their photofission cross sections per nucleon $\sigma_{\gamma F}/A$.

The assumption $W_F \approx 1$ had to be reconsidered after a Novosibirsk group [6] reported that the fission probability for ^{237}Np is about 30% higher than that for ^{238}U in the photon energy range 60–240 MeV. Subsequent measurements performed at the Saskatchewan Accelerator Laboratory (SAL) [7] corroborated these results for the same energy range. We now observe this trend to be true up to 4 GeV.

This experiment was the first measurement performed in Hall B at the Thomas Jefferson National Accelerator Fa-

cility (Jefferson Lab) using the photon-tagging facility [8]. An electron beam is passed through a thin radiator to produce bremsstrahlung. The residual energy of an electron after bremsstrahlung emission is deduced from its measured position in the focal plane of the tagger bending magnet. The two-layer focal-plane detector array has an energy resolution of 0.1% provided by the highly segmented E -counter layer and a time resolution of ~ 1 ns for a given T -counter in coincidence with a fission-fragment detector. By requiring a tight time coincidence between a T -counter and a corresponding E -counter, the background from secondary sources in the tagger focal plane was significantly reduced.

The detector system is able to tag photons with energies from 20% to 95% of the incident electron energy at a single magnetic field setting. Thus, with incident electron beam energies of 0.88, 1.71, and 4.04 GeV, we were able to span the photon energy range from 0.17 to 3.84 GeV. Using these beam energies allowed for sufficient overlap between the energy bites to provide a consistency check of the absolute normalization for different data sets. The difference between the 1.71- and 4.04-GeV data in the overlap region is about 3%. Total fluxes of tagged photons of about 3×10^7 photons/s were used during the measurements.

The fission targets studied in this experiment were ^{237}Np , ^{238}U , ^{235}U , ^{233}U , ^{232}Th , and $^{\text{nat}}\text{Pb}$. Each of these targets consists of a thin layer of ~ 1 mg/cm² of target material deposited on a backing foil (100 μm aluminum for the actinide isotopes and 25 μm Mylar for the lead targets). In order to increase the number of counts per isotope, we used three targets for each of the actinides and seven for lead. For the latter, the effective thickness was further increased by a factor of 1.4 by tilting the targets by 45° with respect to the incident photon beam.

One of the fission fragments produced by the interaction of an incident photon with one of these target nuclei was detected for each event. The fission-fragment detectors are novel low-pressure parallel-plate avalanche detectors (PPADs), which are described in detail elsewhere [9]. The anode plane of each of the PPADs consists of a vertical array of 25- μm diameter gold-plated tungsten-rhenium wires spaced 1 mm apart. The cathode plane, positioned 3 mm from the anode, is a 25- μm foil of aluminized Mylar. The ionization gas is isobutane. At our operating parameters (15 Torr and 750 V) these devices are 97.5% efficient, where the small inefficiency is due to the lack of total transparency of the anode wire plane.

Each fission-target foil was mounted on a frame and placed in front of its own PPAD at a distance of 1.3 cm for the actinide targets and 0.4 cm for lead. The acceptance was well defined by circular 4-cm-diameter collimators located between the target foil and the anode plane. All of these target-detector combinations shared the same reaction chamber and thus the same gas pressure. The reaction chamber was placed in the beam line immediately downstream of the tagger magnet. This arrangement has the important advantage of enabling us to study all of the fission targets simultaneously, under exactly the same experimental conditions. The trigger for the experiment was given by the OR of all the PPAD signals. At typical event rates of ~ 150 Hz, the chance of having two PPADs in accidental coincidence was less than 0.1%.

The PPADs provide good separation between alpha particles and fission fragments, as determined by the pulse-height distribution in the analog-to-digital converter. The time coincidence between a PPAD signal and the associated electron detected in the focal plane results in a peak

in the tagger time-to-digital converter spectrum. Random coincidences due to events caused by untagged photons and by radioactive decay products were subtracted from the coincidence peak to give the yield of fission-fragment events.

The dominant sources of systematic uncertainty are the target thicknesses [10] and the photon-tagging efficiency. Each contributes less than 5% and neither depends significantly on the photon energy. Uncertainties in collimator position and anode wire blockage combine for an additional 2%. This leads to an overall systematic uncertainty of 7% in both the absolute and relative cross sections. In the latter the cancellation of the flux uncertainty is compensated by the additional thickness uncertainty owing to the presence of two targets.

Figure 1 shows our results for the ^{237}Np , ^{238}U , and ^{232}Th absolute photofission cross sections per nucleon $\sigma_{\gamma F}/A$ as a function of the incident photon energy. The error bars reflect statistical uncertainties only. The previously existing photofission data for these three isotopes are also shown. The present data are in good agreement at low energies with the data from Refs. [6,7]. Our ^{238}U data agree well with the average of the Mainz [11] and Frascati [12] data from the Δ -resonance region up to about 800 MeV. In the same energy region our ^{232}Th data agree with the Frascati [13] data.

In Fig. 2 we present a comparison between the photofission data for ^{237}Np , ^{238}U , and ^{232}Th and the existing Pb photoabsorption data [5,14–16]. The photofission data include the data presented in this paper as well as previous data from [6,7,11–13]. Both $\sigma_{\gamma F}$ and $\sigma_{\gamma A}$ data were fitted using a modified Breit-Wigner formula. We note that the only low-energy data on Pb [14]

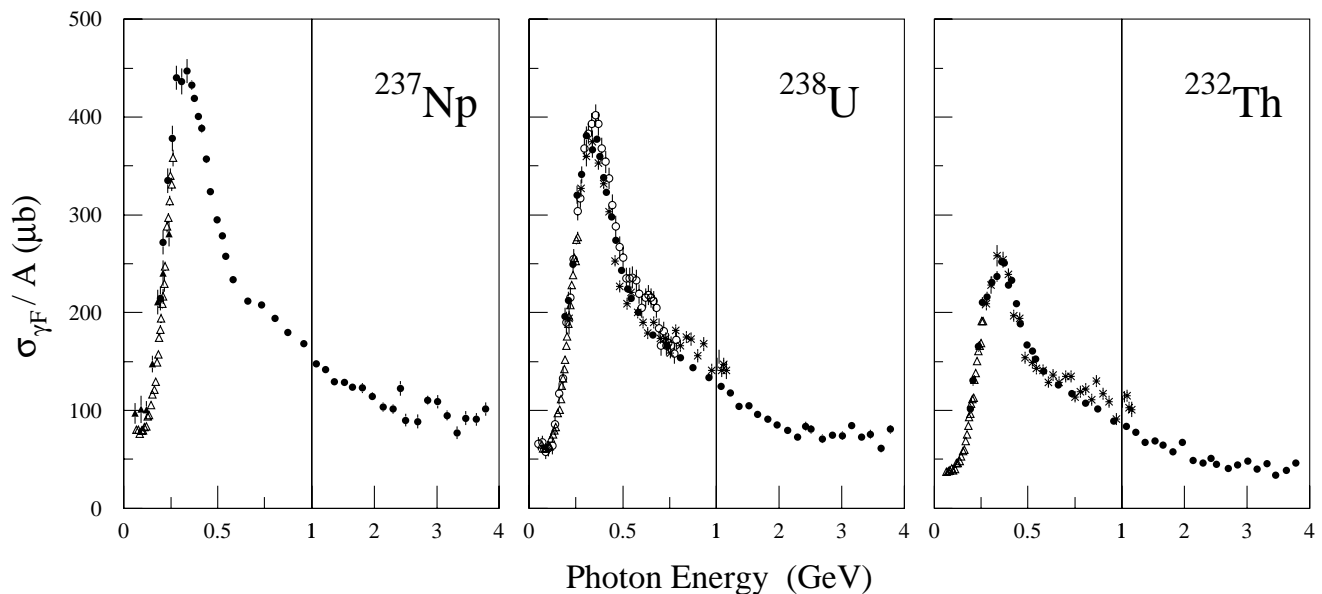


FIG. 1. Absolute photofission cross sections per nucleon as a function of the incident photon energy for ^{237}Np , ^{238}U , and ^{232}Th . Note that the energy region below 1 GeV has been expanded. The present results (closed circles) are compared with previous results: (open triangles) [7], (closed triangles) [6], (open circles) [11], and (stars) [12,13].

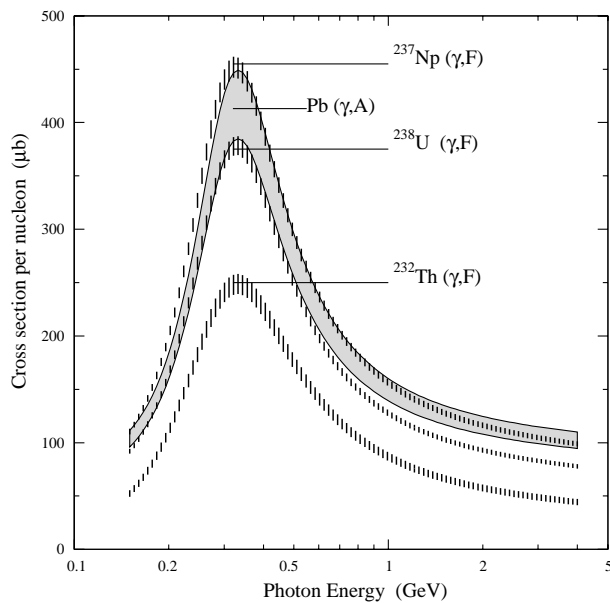


FIG. 2. Photofission cross sections per nucleon for ^{237}Np , ^{238}U , and ^{232}Th (bar bands) and photoabsorption cross section per nucleon for Pb (gray band). The bands represent fits to the existing data, present and previous, for Np [6,7], U [6,7,11,12], Th [7,13], and Pb [5,14–16] (see text). The band widths represent the uncertainties in the fits. The energy scale is logarithmic, for clarity at the lower energies.

should be regarded as a lower limit since it includes only (γ, xn) cross sections, where $x \geq 2$, and hence does not include any of the (γ, n) , (γ, p) , (γ, α) , (γ, pn) , or $(\gamma, \alpha n)$ channels. One can see that $\sigma_{\gamma F}/A$ for ^{237}Np is a few percent higher than $\sigma_{\gamma A}/A$ for Pb only below the Δ peak, and is in very good agreement at higher energies.

Using the highest cross section as a reference, namely that for ^{237}Np , we show in Fig. 3 the photofission cross sections per nucleon for ^{238}U and ^{232}Th relative to that for ^{237}Np , as a function of the incident photon energy. One can see that the probability for ^{238}U to undergo fission is about 20% smaller than that for ^{237}Np , while ^{232}Th fissions with about half the probability of ^{237}Np .

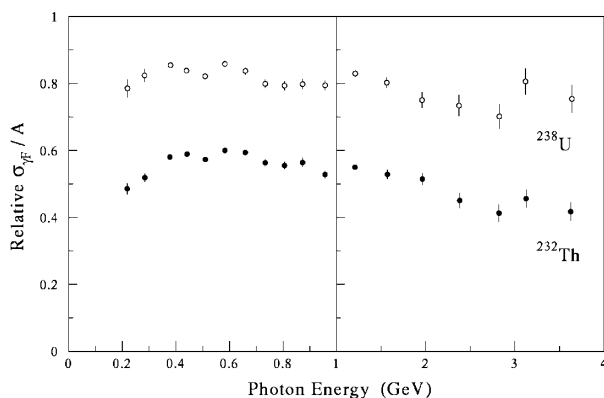


FIG. 3. Photofission cross sections per nucleon relative to ^{237}Np as a function of the incident photon energy for ^{238}U and ^{232}Th . The energy region below 1 GeV has been expanded.

The energy dependence of the relative cross sections appears to be almost flat, suggesting that a common mechanism is responsible for the photofission process. This suggests in turn that the two-step cascade-evaporation model [17], which is used to explain the fission process at intermediate energies [18], is also valid in the 1–4 GeV region. According to this model, the incident projectile initiates an intranuclear cascade. On a very short time scale (10^{-22} s), some of the excited particles exit the nucleus, carrying away both energy and charge (preequilibrium emission). The remaining energy is distributed among the other nucleons to form a residual compound nucleus in a highly excited state. After reaching equilibrium, the compound nucleus, over an extended time period (10^{-19} s), loses its excitation energy either by evaporating particles (mostly neutrons) or by undergoing fission at any stage in the process.

Figure 4 depicts these relative cross sections as a function of the fissility parameter Z^2/A . The vertical bars represent the range spanned by the relative cross sections over the energy range of the present experiment. Insofar as the logarithmic dependence of the relative cross section approaches an asymptotic value, one can infer that the fission probability approaches unity. This means that for ^{237}Np the fission probability, while perhaps not reaching unity, probably is close to unity.

In the energy range available at Jefferson Lab, photoabsorption leads to the excitation of bound nucleons and the production of baryon resonances which behave quite differently inside the nuclear medium, compared with the case for free nucleons. The D_{13} and F_{15} resonances, clearly seen in the photoabsorption on the proton and the deuteron [19], and still seen in ^3He [20], are not observed in the total cross sections for $A \geq 4$ nuclei. Photoabsorption measurements have been done for Li, C, Al, Cu, Sn, and Pb [15], and photofission measurements for Th [13] and U [11,12]. As expected from most previous data, the present photofission cross sections exhibit no prominent resonance structure above the Δ resonance.

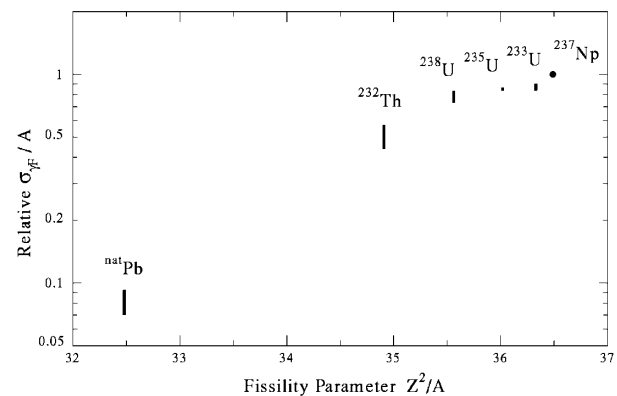


FIG. 4. Photofission cross sections per nucleon relative to ^{237}Np as a function of the fissility parameter Z^2/A . The vertical bars represent the range spanned by the relative cross sections over the energy range of the present experiment.

Figure 5 shows the ratios of the photofission cross sections for ^{237}Np , ^{238}U , ^{232}Th , and the corresponding cross sections for the sum of the protons and neutrons [19] in each of these nuclei. Two data points [21] for the photoabsorption cross section for ^{238}U are shown for comparison. In order to interpret these data, we recall that photons with incident energies above the resonance region begin to exhibit hadronic behavior, and the total cross section starts to show the onset of the “shadowing” effect [22,23]. Since this behavior results in greatly increased interaction strength for the photon with hadronic matter, shadowing in nuclei manifests itself as the total photoabsorption cross section gradually evolves from purely volume absorption ($\propto A$) towards purely surface absorption ($\propto A^{2/3}$). This effect can be quantified by use of the expression $A_{\text{eff}}/A = \sigma_{\gamma A}/(Z\sigma_{\gamma p} + N\sigma_{\gamma n})$, where A_{eff} represents the effective number of nucleons seen by the incident photon, while $\sigma_{\gamma p}$ and $\sigma_{\gamma n}$ are the free-nucleon photoabsorption cross sections for the proton and the neutron, respectively.

We have seen that $\sigma_{\gamma F}$ is smaller than $\sigma_{\gamma A}$ for the three uranium isotopes, for Th, and for Pb. Thus, we cannot use the photofission cross section to measure the shadowing effect, except perhaps for the case of ^{237}Np (if we assume that its photofission probability is equal to unity, as suggested by Fig. 2). If we make this assumption, we observe the onset of shadowing below 1.5 GeV, such that A_{eff}/A decreases to $\sim 75\%$ at 3.6 GeV, as shown in Fig. 5. It is also clear that $\sigma_{\gamma F}$ for ^{238}U is much less than $\sigma_{\gamma A}$, while $\sigma_{\gamma F}$ for ^{237}Np is not. This trend supports the hypothesis that the fission probability for ^{237}Np is close to 100%, and is quite consistent with the relative fission cross sections of Fig. 4, which appear to be approaching an asymptote at the Z^2/A value of ^{237}Np .

In summary, we have performed a simultaneous measurement of the total photofission cross sections for ^{237}Np , three uranium isotopes, ^{232}Th , and $^{\text{nat}}\text{Pb}$ in the photon energy range from 0.17 to 3.84 GeV. The relative photofission cross sections show that, of these nuclei, ^{237}Np has

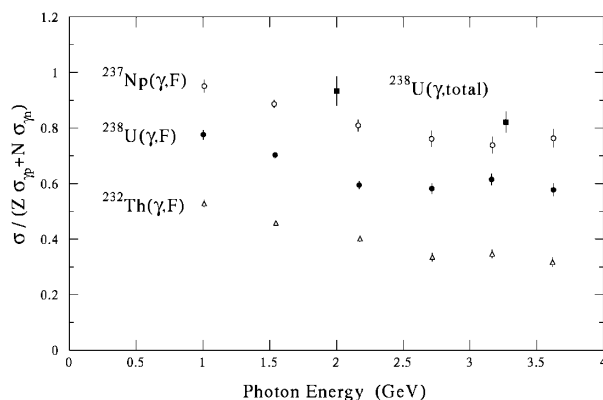


FIG. 5. Ratio of the photofission cross sections for ^{237}Np , ^{238}U , and ^{232}Th and the corresponding total cross sections for the sum of the protons and neutrons [19] in each of these nuclei. Two data points (closed squares) [21] for the total photoabsorption cross section for ^{238}U are shown for comparison.

the highest probability to undergo fission, and that the fission probability for ^{238}U , which often has been assumed to be equal to unity, is in fact only about 80% of that of ^{237}Np , and does not depend strongly on the incident photon energy up to 4 GeV. These results invalidate the use of the photofission reaction alone to determine the total photoabsorption cross section for heavy nuclei; a detailed investigation of *all* of the exit channels following photoabsorption is required to understand completely the microscopic mechanism governing this process.

This work was supported in part by the U.S. Department of Energy under Grant No. DE-FG02-95ER40901 and by the National Science Foundation. W.R. Dodge, V.G. Nedorezov, and A.S. Sudov contributed during various stages of preparing the experimental equipment. We thank those who took shifts during the nine days of data taking: D. Branford, B. Carnahan, K.S. Dhuga, M. Dugger, J.T. O'Brien, B.G. Ritchie, and I.I. Strakovsky. We were aided in handling the data-acquisition system by the expertise of S.P. Barrow. We would like to acknowledge the contribution of the Jefferson Lab staff, especially B.A. Mecking and E.S. Smith, for their advice and support. Finally, special thanks are due to G.V. O'Rielly for constructive discussions during the data analysis.

*Present address: Department of Physics, Univ. of Texas at El Paso, El Paso, TX 79968.

†Present address: Department of Physics, Universidad de los Andes, Bogota, Colombia.

‡Deceased.

- [1] J. Ahrens *et al.*, Phys. Lett. **146B**, 303 (1984).
- [2] Th. Frommhold *et al.*, Phys. Lett. B **295**, 28 (1992).
- [3] J. Ahrens, Nucl. Phys. **A446**, 229c (1985).
- [4] J. Ahrens and J.S. O'Connell, Comments Nucl. Part. Phys. **14**, 245 (1985).
- [5] V. Muccifora *et al.*, Phys. Rev. C **60**, 064616 (1999).
- [6] A.S. Iljinov *et al.*, Nucl. Phys. **A539**, 263 (1992).
- [7] J.C. Sanabria *et al.*, Phys. Rev. C **61**, 034604 (2000).
- [8] D.I. Sober *et al.*, Nucl. Instrum. Methods Phys. Res., Sect. A **440**, 263 (2000).
- [9] J.C. Sanabria *et al.*, Nucl. Instrum. Methods Phys. Res., Sect. A **441**, 525 (2000).
- [10] J.C. Sanabria (to be published).
- [11] Th. Frommhold *et al.*, Z. Phys. A **350**, 249 (1994).
- [12] N. Bianchi *et al.*, Phys. Lett. B **299**, 219 (1993).
- [13] N. Bianchi *et al.*, Phys. Rev. C **48**, 1785 (1993).
- [14] C. Chollet *et al.*, Phys. Lett. **127B**, 331 (1983).
- [15] N. Bianchi *et al.*, Phys. Rev. C **54**, 1688 (1996).
- [16] G.R. Brooks *et al.*, Phys. Rev. D **8**, 2826 (1973).
- [17] K. Kikuchi and M. Kawai, *Nuclear Matter and Nuclear Reactions* (North-Holland, Amsterdam, 1968).
- [18] A.S. Iljinov *et al.*, Nucl. Phys. **A617**, 575 (1997).
- [19] T.A. Armstrong *et al.*, Phys. Rev. D **5**, 1640 (1972); Nucl. Phys. **B41**, 445 (1972).
- [20] M. MacCormick *et al.*, Phys. Rev. C **53**, 41 (1996).
- [21] S. Michalowski *et al.*, Phys. Rev. Lett. **39**, 737 (1977).
- [22] W. Weise, Phys. Rep. **13**, 53 (1974).
- [23] T.H. Bauer *et al.*, Rev. Mod. Phys. **50**, 261 (1978).